Journal of Energy and Power Engineering 7 (2013) 1344-1351

Model-Based Fault Detection of a Battery System in a Hybrid Electric Vehicle

S. Andrew Gadsden and Saeid R. Habibi

Department of Mechanical Engineering, McMaster University, Hamilton L8S 4L7, Ontario, Canada

Received: November 01, 2011 / Accepted: February 02, 2012 / Published: July 31, 2013.

Abstract: Recently, a new type of IMM (interacting multiple model) method was introduced based on the relatively new SVSF (smooth variable structure filter), and is referred to as the IMM-SVSF. The SVSF is a type of sliding mode estimator that is formulated in a predictor-corrector fashion. This strategy keeps the estimated state bounded within a region of the true state trajectory, thus creating a stable and robust estimation process. The IMM method may be utilized for fault detection and diagnosis, and is classified as a model-based method. In this paper, for the purposes of fault detection, the IMM-SVSF is applied through simulation on a simple battery system which is modeled from a hybrid electric vehicle.

Key words: Battery system, fault detection and diagnosis, interacting multiple model, smooth variable structure filter, Kalman filter.

1. Introduction

Modern control theory relies on reliable state estimates in order to provide accurate and safe control of mechanical and electrical systems. Estimation theory is therefore an important tool for providing accurate state and parameter estimates. The most popular estimation method to date remains the KF (Kalman filter) which was introduced and applied on a number of systems in the 1960s [1, 2]. It yields a statistically optimal solution for linear estimation problems in the presence of Gaussian noise [1]. In other words, based on the available information on the system, it yields the best possible solution in terms of estimation error [3]. The KF assumes that the system model is known and linear, the system and measurement noises are white, and the states have initial conditions and are modeled as random variables with known means and variances [4, 5]. However, these assumptions do not always hold in real applications. If one of these assumptions is violated, the KF performance becomes sub-optimal and could potentially become unstable [6].

As presented in Ref. [7], the ability to detect and diagnose faults is essential for the safe and reliable control of mechanical and electrical systems. In the presence of a fault, the system behaviour may become unpredictable, resulting in a loss of control which can cause unwanted downtime as well as damage to the system. There are two main types of methods to detect and diagnose faults: signal-based and model-based [8]. Signal-based fault detection methods typically use thresholds to extract information from available measurements [9, 10]. This information is then used to determine if a fault is presented. Model-based methods, as the name suggests, make use of faults which can be modeled, typically through system identification. This type of fault detection and diagnosis is popular when well-defined models can be created and utilized.

The IMM (interacting multiple model) strategy makes use of a finite number of models, and is associated with filters that run in parallel. The output from each filter includes the state estimate, the

Corresponding author: S. Andrew Gadsden, postdoctoral fellow and researcher, research fields: control systems theory, mechatronics, state and parameter estimation, aerospace systems. E-mail: gadsden@mcmaster.ca.

covariance, and the likelihood calculation (which is a function of the measurement error and innovation covariance). The output from the filters is used to calculate mode probabilities, which gives an indication of how close the filter model is to the true model. The IMM method has been successfully applied on mechanical and electrical systems for fault detection and diagnosis [4, 11]. Typically, the IMM implements the KF strategy for determining the state estimates. However, this paper studies the results of using the SVSF (smooth variable structure filter) instead of the KF, as applied on a HEV (hybrid electric vehicle) battery system.

2. Filtering Strategies

2.1 Kalman Filter

In 1960, Rudolph Kalman presented a new approach to linear filtering and prediction problems, which would later become known as the KF (Kalman filter) [1]. This method was successfully applied by NASA for their lunar and Apollo missions, and quickly became the "workhorse" of estimation [5, 12]. The KF yields a statistically optimal solution for linear estimation problems in the presence of Gaussian noise. The KF is a model based method, derived in the time domain and a discrete-time setting. A continuous-time version was developed by Kalman and Bucy, and is consequently referred to as the Kalman-Bucy filter [2].

Like many other filters, the KF is formulated in a predictor-corrector manner. The states are first estimated using the system model and input, termed as a priori estimates, meaning "prior to" knowledge of the observations. A correction term is then added based on the innovation (also called residuals or measurement errors), thus forming the updated or a posteriori (meaning "subsequent to" the observations) state estimates. The KF has been broadly applied to problems covering state and parameter estimation, signal processing, target tracking, fault detection and diagnosis, and even financial analysis [13, 14]. The success of the KF comes from the optimality of the Kalman gain in minimizing the trace of the a posteriori state error covariance matrix [1]. The trace is taken because it represents the state error vector in the estimation process [6].

The following five equations form the core of the KF algorithm, and are used in an iterative fashion. Eqs. (1) and (2) define a priori state estimate $\hat{x}_{k+1|k}$ based on knowledge of the system A and previous state estimate $\hat{x}_{k|k}$, and the corresponding state error covariance matrix $P_{k+1|k}$, respectively:

$$\hat{x}_{k+1|k} = A\hat{x}_{k|k} + Bu_k \tag{1}$$

$$P_{k+1|k} = AP_{k|k}A^T + Q_k \tag{2}$$

The Kalman gain K_{k+1} is defined by Eq. (3), and is used to update the state estimate $\hat{x}_{k+1|k+1}$ as shown in Eq. (4). The gain makes use of an innovation covariance S_{k+1}, which is defined as the inverse term found in Eq. (3).

$$K_{k+1} = P_{k+1|k}C^T\left(CP_{k+1|k}C^T + R_{k+1}\right)^{-1} \tag{3}$$

$$\hat{x}_{k+1|k+1} = \hat{x}_{k+1|k} + K_{k+1}\left(z_{k+1} - C\hat{x}_{k+1|k}\right) \tag{4}$$

The posteriori state error covariance matrix $P_{k+1|k+1}$ is then calculated by Eq. (5), and is used iteratively, as per Eq. (2):

$$P_{k+1|k+1} = (I - K_{k+1}C)P_{k+1|k} \tag{5}$$

The derivation of the KF is well documented, with details available in Refs. [1, 3, 6]. The optimality of the KF comes at a price of stability and robustness. The KF assumes that the system model is known and linear, the system and measurement noises are white, and the states have initial conditions with known means and variances [5]. However, the previous assumptions do not always hold in real applications. If these assumptions are violated, the KF yields suboptimal results and can become unstable [15]. Furthermore, the KF is sensitive to computer precision and the complexity of computations involving matrix inversions [16].

2.2 Smooth Variable Structure Filter

The SVSF (smooth variable structure filter) was presented in 2007 [17]. The SVSF strategy is also a predictor-corrector estimator based on sliding mode concepts, and can be applied on both linear or nonlinear systems and measurements. As shown in Fig. 1, and similar to the VSF, it utilizes a switching gain to converge the estimates to within a boundary of the true state values (i.e., existence subspace) [17]. The SVSF has been shown to be stable and robust to modeling uncertainties and noise, when given an upper bound on the level of un-modeled dynamics and noise [17, 18].

The origin of the SVSF name comes from the requirement that the system is differentiable (or "smooth") [17, 19]. Furthermore, it is assumed that the system under consideration is observable [17]. The following process for the SVSF estimation strategy, as applied to a nonlinear system with a linear measurement equation, should be considered. The predicted state estimates $\hat{x}_{k+1|k}$ are first calculated as follows:

$$\hat{x}_{k+1|k} = \hat{f}\left(\hat{x}_{k|k}, u_k\right) \tag{6}$$

Utilizing the predicted state estimates $\hat{x}_{k+1|k}$, the corresponding predicted measurements $\hat{z}_{k+1|k}$ and measurement errors $e_{z,k+1|k}$ may be calculated:

$$\hat{z}_{k+1|k} = C\hat{x}_{k+1|k} \tag{7}$$

$$e_{z,k+1|k} = z_{k+1} - \hat{z}_{k+1|k} \tag{8}$$

Next, the SVSF gain is calculated as follows [17]:

$$K_{k+1}^{SVSF} = C^{+}\left(\left|e_{z,k+1|k}\right| + \gamma\left|e_{z,k|k}\right|\right)sat\left(\frac{e_{z,k+1|k}}{\psi}\right) \tag{9}$$

The SVSF gain is a function of: a priori and a posteriori measurement errors $e_{z,k+1|k}$ and $e_{z,k|k}$; the smoothing boundary layer widths ψ; the "SVSF" memory or convergence rate γ with elements $0 < \gamma_{ii} \leq 1$; and the linear measurement matrix C. The SVSF gain is used to refine the state estimates as follows:

$$\hat{x}_{k+1|k+1} = \hat{x}_{k+1|k} + K_{k+1}^{SVSF} \tag{10}$$

Next, the updated measurement estimates $\hat{z}_{k+1|k+1}$ and corresponding errors $e_{z,k+1|k+1}$ are calculated:

$$\hat{z}_{k+1|k+1} = C\hat{x}_{k+1|k+1} \tag{11}$$

$$e_{z,k+1|k+1} = z_{k+1} - \hat{z}_{k+1|k+1} \tag{12}$$

The SVSF process may be summarized by Eq. (6) through Eq. (12), and is repeated iteratively. According to Ref. [17], the estimation process is stable and convergent if the following condition is satisfied:

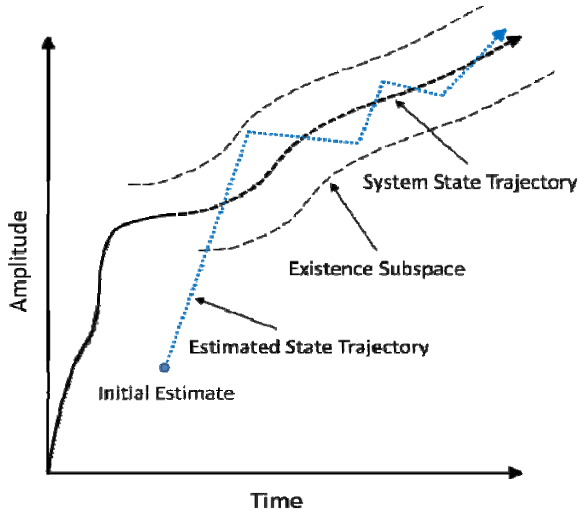

Fig. 1 The SVSF estimation strategy [20]. Starting from some initial value, the state estimate is forced by a switching gain to within a region referred to as the existence subspace.

$$\left|e_{k|k}\right| > \left|e_{k+1|k+1}\right| \tag{13}$$

The proof, as described in Refs. [17, 19], yields the derivation of the SVSF gain from Eq. (13). The SVSF results in the state estimates converging to the state trajectory. Thereafter, it switches back and forth across the state trajectory within a region referred to as the existence subspace. The existence subspace represents the amount of uncertainties that are presented in the estimation process, in terms of modeling errors or the presence of noise. The width of the existence space β is a function of the uncertain dynamics associated with the inaccuracy of the internal model of the filter as well as the measurement model, and varies with time [17]. Typically, this value is not exactly known, but an upper bound may be selected based on a priori knowledge.

Once within the existence boundary subspace, the estimated states are forced (by the SVSF gain) to switch back and forth along the true state trajectory. The high-frequency switching caused by the SVSF gain is referred to as chattering, and in most cases, is undesirable for obtaining accurate estimates [17]. However, the effects of chattering may be minimized by the introduction of a smoothing boundary layer ψ. The selection of the smoothing boundary layer width reflects the level of uncertainties in the filter and the disturbances (i.e., system and measurement noise, and un-modeled dynamics).

When the smoothing boundary layer is defined larger than the existence subspace boundary, the estimated state trajectory is smoothed. However, when the smoothing term is too small, chattering remains due to the uncertainties being underestimated. The smoothing boundary layer ψ modifies the SVSF gain as follows [17]:

$$K_{k+1}^{SVSF} = C^{+}\left(\left|e_{z,k+1|k}\right| + \gamma\left|e_{z,k|k}\right|\right)sat\left(e_{z,k+1|k}/\psi\right) \quad (14)$$

The SVSF estimation process is inherently robust and stable to modeling uncertainties due to the switching effect of the gain. This makes for a powerful estimation strategy, particularly when the system is not well known. It is noted that for systems that have fewer measurements than states, a "reduced order" approach is taken to formulate a full measurement matrix [17, 20]. Essentially, "artificial measurements" are created and used throughout the estimation process.

3. The IMM-SVSF Strategy

The IMM was implemented in Ref. [4]. The concept is shown in Fig. 2. The IMM-SVSF estimator consists of five main steps: calculation of the mixing probabilities, mixing stage, mode-matched filtering via the SVSF, mode probability update, and state estimate and covariance combination. The first step involves calculating the mixing probabilities $\mu_{i|j,k|k}$ (i.e., the probability of the system currently in mode i, and switching to mode j at the next step). These are calculated using the following two equations [4]:

$$\mu_{i|j,k|k} = \frac{1}{\bar{c}_j} p_{ij}\mu_{i,k} \quad (15)$$

$$\bar{c}_j = \sum_{i=1}^{r} p_{ij}\,\mu_{i,k} \quad (16)$$

It is noted that p_{ij} refers to the mode transition probabilities, and is a designer parameter. It is noted that $\mu_{i,k}$ refers to the probability of the mode i being correct (with values between 0 and 1), and differs from the mixing probabilities $\mu_{i|j,k|k}$. This notation is standard, and is found in Ref. [4]. The mixing probabilities $\mu_{i|j,k|k}$ are used in the mixing stage, next. In addition to the mixing probabilities, the previous mode-matched states $\hat{x}_{i,k|k}$ and covariance's $P_{i,k|k}$ are

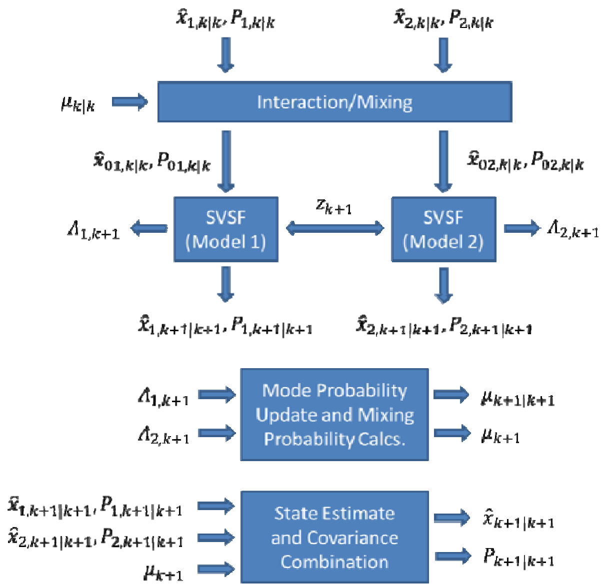

Fig. 2 The IMM-SVSF method, adapted from Ref. [4]. The SVSF estimation strategy may be applied on a finite number of models. As an example, this figure shows two models. Essentially, a mode probability is calculated for each filter and operating mode, and weighted state estimates are created.

also used to calculate the mixed initial conditions (states and covariance) for the filter matched to M_j (which consists of A_j and B_j). The mixed initial conditions are found respectively as follows [4]:

$$\hat{x}_{0j,k|k} = \sum_{i=1}^{r} \hat{x}_{i,k|k}\mu_{i|j,k|k} \quad (17)$$

$$P_{0j,k|k} = \sum_{i=1}^{r} \mu_{i|j,k|k}\left\{P_{i,k|k} + \left(\hat{x}_{i,k|k} - \hat{x}_{0j,k|k}\right)\left(\hat{x}_{i,k|k} - \hat{x}_{0j,k|k}\right)^{T}\right\} \quad (18)$$

The next step involves mode-matched filtering via the SVSF, which involves using Eqs. (17) and (18) as inputs to the SVSF matched to M_j. Each SVSF also uses the measurement z_{k+1} and input to the system u_k.

The SVSF was adapted to include a covariance function, and is presented in Ref. [21]. The modified SVSF prediction stage (for linear systems) is as follows: the state estimates $\hat{x}_{0j,k|k}$ (17) and corresponding covariance $P_{0j,k|k}$ (18) for each model j are used to predict the state estimate $\hat{x}_{j,k+1|k}$ (19) and calculate the priori state error covariance matrix $P_{j,k+1|k}$ (20).

$$\hat{x}_{j,k+1|k} = A_j\hat{x}_{0j,k|k} + B_j u_k \quad (19)$$

$$P_{j,k+1|k} = A_j P_{k|k}^{0j} A_j^{T} + Q_k \quad (20)$$

From Eqs. (19) and (20), the mode-matched innovation covariance $S_{j,k+1|k}$ (21) and mode-matched priori measurement error $e_{j,z,k+1|k}$ (22) are calculated.

$$S_{j,k+1|k} = C_j P_{j,k+1|k} C_j^T + R_{k+1} \tag{21}$$

$$e_{j,z,k+1|k} = z_{k+1} - C_j \hat{x}_{j,k+1|k} \tag{22}$$

The update stage is defined by the following four equations. The mode-matched SVSF gain $K_{j,k+1}$ is calculated in Eq. (23) and used to update the state estimates $\hat{x}_{j,k+1|k+1}$ (24).

$$K_{j,k+1} = C_j^{+} diag\left[\left(\left|e_{j,z,k+1|k}\right| + \gamma_j \left|e_{j,z,k|k}\right|\right) sat\left(\bar{\psi}_j^{-1} e_{j,z,k+1|k}\right)\right] diag\left(e_{j,z,k+1|k}\right)^{-1} \tag{23}$$

$$\hat{x}_{j,k+1|k+1} = \hat{x}_{j,k+1|k} + K_{j,k+1} e_{j,z,k+1|k} \tag{24}$$

The corresponding state error covariance matrix $P_{j,k+1|k+1}$ is then calculated in Eq. (25) and the posteriori measurement error $e_{j,z,k+1|k+1}$ may be found in Eq. (26).

$$P_{j,k+1|k+1} = \left(I - K_{j,k+1} C_j\right) P_{j,k+1|k} \left(I - K_{j,k+1} C_j\right)^T + K_{j,k+1} R_{k+1} K_{j,k+1}^T \tag{25}$$

$$e_{j,z,k+1|k+1} = z_{k+1} - C_j \hat{x}_{j,k+1|k+1} \tag{26}$$

Based on the mode-matched innovation matrix $S_{j,k+1|k}$ (21) and the mode-matched a priori measurement error $e_{j,z,k+1|k}$ (22), a corresponding mode-matched likelihood function $\Lambda_{j,k+1}$ based on the SVSF estimation method may be calculated, as follows [4]:

$$\Lambda_{j,k+1} = \mathcal{N}\left(z_{k+1}; \hat{z}_{j,k+1|k}, S_{j,k+1}\right) \tag{27}$$

Eq. (27) may be solved as follows [4]:

$$\Lambda_{j,k+1} = \frac{1}{\sqrt{\left|2\pi S_{j,k+1}\right|}} exp\left(\frac{-\frac{1}{2} e_{j,z,k+1|k}^T e_{j,z,k+1|k}}{S_{j,k+1}}\right) \tag{28}$$

Utilizing the mode-matched likelihood functions $\Lambda_{j,k+1}$, the mode probability $\mu_{j,k}$ may be updated by [4]:

$$\mu_{j,k} = \frac{1}{c} \Lambda_{j,k+1} \sum_{i=1}^{r} p_{ij}\, \mu_{i,k} \tag{29}$$

where the normalizing constant is defined as [4]:

$$c = \sum_{j=1}^{r} \Lambda_{j,k+1} \sum_{i=1}^{r} p_{ij}\, \mu_{i,k} \tag{30}$$

Finally, the overall IMM-SVSF state estimates $\hat{x}_{k+1|k+1}$ (31) and corresponding covariance $P_{k+1|k+1}$ (32) are calculated:

$$\hat{x}_{k+1|k+1} = \sum_{j=1}^{r} \mu_{j,k+1} \hat{x}_{j,k+1|k+1} \tag{31}$$

$$P_{k+1|k+1} = \sum_{j=1}^{r} \mu_{j,k+1} \{P_{j,k+1|k+1} + \left(\hat{x}_{j,k+1|k+1} - \hat{x}_{k+1|k+1}\right)\left(\hat{x}_{j,k+1|k+1} - \hat{x}_{k+1|k+1}\right)^T\} \tag{32}$$

The formulation of the IMM-SVSF may be summarized by Eq. (15) through Eq. (32), where there are $i, j = 1, \dots, r$ models. It is noted that Eqs. (31) and (32) are only used for output purposes, and are not part of the algorithm recursions [4]. Furthermore, it is noted that the IMM-KF strategy is the same process as above but Eq. (19) through Eq. (26) are replaced with the KF prediction and update equations.

4. HEV Battery Model

A variety of batteries have been studied in literature, most notably lead-acid and lithium-ion batteries [22-26]. Lead-acid batteries are the oldest type of rechargeable batteries, and are most commonly found in motor vehicles. Lithium-ion batteries are also a form of rechargeable battery, which contain lithium in its positive electrode (cathode). These batteries are usually found in portable consumer electronics (i.e., laptops or notebooks) due to particularly high energy-to-weight ratios, slow self-discharge, and a lack of memory effect (i.e., where a battery loses its maximum energy capacity over time) [23].

In recent years, lithium-ion batteries have slowly entered the hybrid electric vehicle market, due to the fact that they offer better energy density compared to standard batteries [27].

The operation of batteries may be studied by using the ADVISOR (advanced vehicle simulator), which was written in MATLAB and Simulink by the US Department of Energy and the National Renewable Energy Laboratory [28-30]. ADVISOR is used for the analysis of performance and fuel economy of three vehicle types: conventional, electric, and hybrid vehicles [28]. In 2001, the RC (resistance-capacitance) battery model was first implemented in ADVISOR [31]. The electrical model consists of three resistors (R_e, R_c, and R_t) and two capacitors (C_b and C_c). The first capacitor (C_b) represents the capability of the battery to chemically store a charge, and the second capacitor (C_c) represents the surface effects of a cell [30]. The resistances and capacitances vary with changing SOC and temperature (T) [30].

ADVISOR offers two different datasets for the RC battery model: lithium-ion and nickel-metal hydride chemistries. For the purposes of this study, the lithium-ion chemistry was used in conjunction with the RC battery model.

A standard model of a parallel hybrid electric vehicle referred to within ADVISOR as the Annex VII PHEV was used for this study. This model has been developed by the IEA (International Energy Agency), which is an international research community for the development and commercialization of hybrid and electric vehicles [32]. The model is based on data obtained from published sources and national (U.S.) research test data [28]. The battery system of the HEV represents the battery pack which stores energy on board the HEV. The system accepts a power request, and returns the available power from the battery, as well as the SOC, voltage and current [28].

The equation that describes the system voltages may be derived from the RC battery model, and is defined as follows:

$$\begin{bmatrix} V_{C_b,k+1} \\ V_{C_c,k+1} \end{bmatrix} = \begin{bmatrix} -\frac{T_s}{C_b(R_e+R_c)}+1 & \frac{T_sR_c}{C_b(R_e+R_c)} \\ \frac{T_sR_e}{C_c(R_e+R_c)} & -\frac{T_s}{C_c(R_e+R_c)}+1 \end{bmatrix} \begin{bmatrix} V_{C_b,k} \\ V_{C_c,k} \end{bmatrix} + \begin{bmatrix} \frac{T_sR_c}{C_b(R_e+R_c)} \\ \frac{T_sR_e}{C_c(R_e+R_c)} \end{bmatrix} I_{S_k} \tag{33}$$

For the purposes of fault detection of the battery, the voltages V_{Cb} and V_{Cc} are treated as states. Normal parameter values were selected from the ADVISOR model. Two faults were designed to represent a fault in one of the capacitors or the resistors.

5. Simulation Results

Both the IMM-KF and IMM-SVSF strategies were applied on a simulated battery model with injected faults. Consider the following scenario: normal operation for the first 10 seconds, followed by a capacitor fault for 5 seconds, then normal operation for another 15 seconds, and finally a resistor fault for the last 10 seconds. The system and measurement noise covariances are defined respectively as follows:

$$Q = 10^{-9} \times diag([1 \quad 1]) \tag{34}$$

$$R = 10^{-6} \times diag([1 \quad 1]) \tag{35}$$

Figs. 3-5 show the mode probabilities for normal operation, and the presence of the two faults. Essentially, it is ideal to follow the true mode probability. Although both strategies were able to correctly identify the mode of operation, the IMM-SVSF strategy was able to provide a more accurate determination. For example, between 15 and 30 seconds, the IMM-SVSF determined with roughly 90% that the battery system was operating normally. However, the IMM-KF strategy had a significantly smaller (about 30% less) probability of detection.

6. Conclusions

This short paper provided an overview of a combined IMM (interacting multiple model) method with the relatively new SVSF (smooth variable structure filter). A very simple battery model used in a HEV system was implemented and studied. Two artificial faults were generated and used in a simulation. The results demonstrate that the new model-based strategy referred to as the IMM-SVSF works more effectively than the popular IMM-KF. Future work will

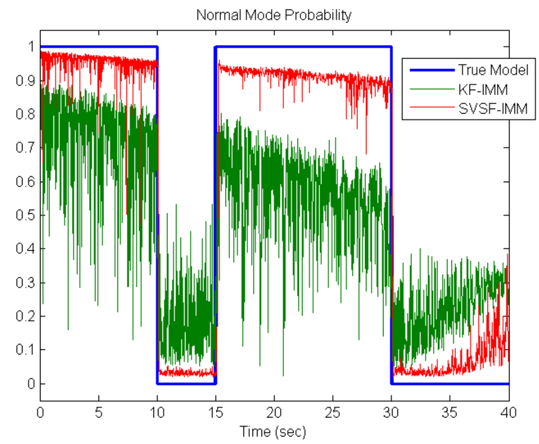

Fig. 3 Normal mode probability for the HEV battery model simulation. The solid blue line represents the true model.

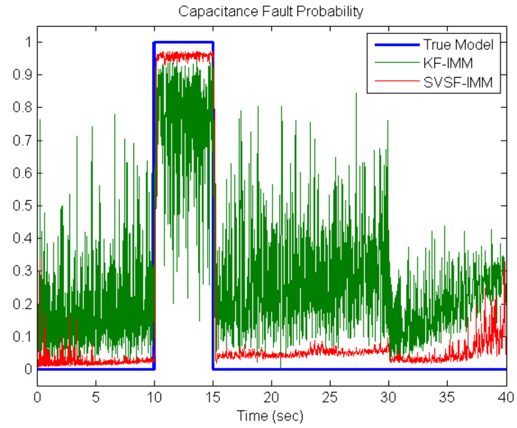

Fig. 4 Capacitance fault probability results for the HEV battery simulation.

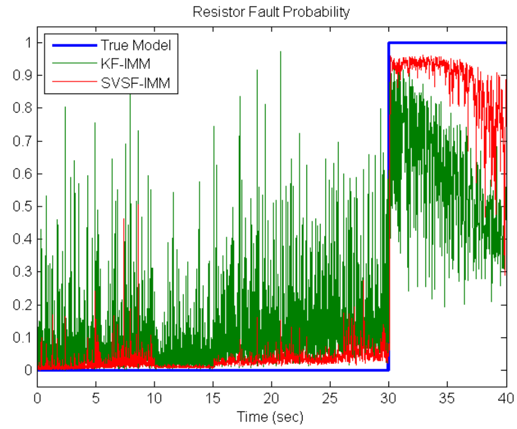

Fig. 5 Resistor fault probability results for the HEV battery simulation.

involve studying a more difficult problem, including varying degrees of faults.

References

[1] R.E. Kalman, A new approach to linear filtering and prediction problems, Journal of Basic Engineering 82 (1960) 35-45.

[2] R. Kalman, R. Bucy, New results in linear filtering and prediction theory, ASME Journal of Basic Engineering 83 (1961) 95-108.

[3] B.D.O. Anderson, J.B. Moore, Optimal Filtering, Prentice-Hall, Englewood Cliffs, NJ, 1979.

[4] Y. Bar-Shalom, X.R. Li, T. Kirubarajan, Estimation with Applications to Tracking and NAVIgation, John Wiley & Sons, Inc., USA, 2001.

[5] D. Simon, Optimal State Estimation: Kalman, H-Infinity, and Nonlinear Approaches, Wiley-Interscience, 2006.

[6] A. Gelb, Applied Optimal Estimation, MIT Press, Cambridge, MA, 1974.

[7] S.A. Gadsden, K.R. McCullough, S.R. Habibi, Fault detection and diagnosis of an electrohydrostatic actuator using a novel interacting multiple model approach, in: American Control Conference (ACC), San Francisco, California, 2011.

[8] R. Isermann, Model-based fault detection and diagnosis-status and applications, Annual Reviews in Control 29 (1) (2005) 71-85.

[9] Y. Wang, Y. Xing, H. He, An intelligent approach for engine fault diagnosis based on wavelet pre-processing neural network model, in: IEEE International Conference on Information and Automation, Harbin, China, 2010, pp. 576-581.

[10] J. Korbicz, Artificial neural networks in fault diagnosis of dynamical systems, in: IEEE Region 8th International Conference on Computational Technologies in Electrical and Electronics Engineering, Listvyanka, 2010, p. 449.

[11] Y. Zhan, J. Jiang, An interacting multiple-model based fault detection, diagnosis and fault-tolerant control approach, in: 38th IEEE Conference on Decision and Control, Phoenix, AZ, 1999, pp. 3593-3598.

[12] L. McGee, S. Schmidt, Discovery of the Kalman Filter as a Practical Tool for Aerospace and Industry, NASA, Technical Memo 86847, 1985.

[13] B. Ristic, S. Arulampalam, N. Gordon, Beyond the Kalman Filter: Particle Filters for Tracking Applications, Artech House, Boston, 2004.

[14] S. Haykin, Kalman Filtering and Neural Networks, John Wiley and Sons, Inc., New York, USA, 2001.

[15] S.J. Julier, J.K. Ulhmann, H.F. Durrant-Whyte, A new method for nonlinear transformation of means and covariances in filters and estimators, IEEE Transactions on Automatic Control 45 (2000) 472-482.

[16] M.S. Grewal, A.P. Andrews, Kalman Filtering: Theory and Practice Using MATLAB, 3rd ed., John Wiley and Sons, Inc., New York, 2008.

[17] S.R. Habibi, The smooth variable structure filter, Proceedings of the IEEE 95 (5) (2007) 1026-1059.

[18] S.R. Habibi, R. Burton, The variable structure filter, Journal of Dynamic Systems, Measurement, and Control (ASME) 125 (2003) 287-293.

[19] M. Al-Shabi, The general toeplitz/observability SVSF, Ph.D. Thesis, Department of Mechanical Engineering, McMaster University, Hamilton, Ontario, 2011.

[20] S.A. Gadsden, Smooth variable structure filtering: Theory and applications, Ph.D. Thesis, Department of Mechanical Engineering, McMaster University, Hamilton, Ontario, 2011.

[21] D.G. Luenberger, Introduction to Dynamic Systems, John Wiley, USA, 1979.

[22] S.A. Gadsden, S.R. Habibi, A new form of the smooth variable structure filter with a covariance derivation, in:

IEEE Conference on Decision and Control, Atlanta, Georgia, 2010.

[23] B.S. Bhangu, P. Bentley, D.A. Stone, C.M. Bingham, Nonlinear observers for predicting state-of-charge and state-of-health of lead-acid batteries for hybrid-electric vehicles, IEEE Transactions on Vehicular Technology 54 (3) (2005) 783-794.

[24] G.L. Plett, Extended Kalman filtering for battery management systems of lipb-based hev battery packs: Part 1, Background, Journal of Power Sciences 134 (2) (2004) 252-261.

[25] A. Vasebi, S.M.T. Bathaee, M. Partovibakhsh, Predicting state of charge of lead-acid batteries for hybrid electric vehicles by extended Kalman filter, Journal of Energy Conversion and Management 49 (2008) 75-82.

[26] G.L. Plett, Sigma-point Kalman filtering for battery management systems of Li-PB-based HEV battery packs: Part 1, Introduction and state estimation, Journal of Power Sources 161 (2006) 1356-1368.

[27] T. Okoshi, K. Yamada, T. Hirasawa, A. Emori, Battery condition monitoring (BCM) technologies about lead-acid batteries, Journal of Power Sources 158 (2006) 874-878.

[28] J. Voelcker, Lithium batteries take to the road, IEEE Spectrum Magazine 44 (9) (2007) 26-31.

[29] ADVISOR 2004 User's Guide, Advanced Vehicle Labs, 2004.

[30] T. Markel, A. Brooker, T. Hendricks, V. Johnson, K. Kelly, B. Kramer, et al., ADVISOR: A systems analysis tool for advanced vehicle modeling, Journal of Power Sources 110 (2002) 255-266.

[31] V.H. Johnson, Battery performance models in ADVISOR, Journal of Power Sources 110 (2002) 321-329.

[32] V.H. Johnson, M. Zolot, A. Pesaran, Development and validation of a temperature-dependent resistance/capacitance battery model for ADVISOR, in: Proceedings of the 18th Electric Vehicle Symposium, Berlin, Germany, Oct. 2001.

[33] HEV Implementing Agreement, International Energy Agency, 2008.

[34] S.A. Gadsden, S.R. Habibi, Model-based fault detection of a battery system in a hybrid electric vehicle, in: IEEE Vehicle Power and Propulsion Conference (VPPC), Chicago, Illinois, 2011.

[35] S.A. Gadsden, Smooth variable structure filtering: Theory and application, Ph.D. Thesis, 2011.